

# MINIMAL TWIN SURFACES

HAO CHEN

ABSTRACT. We report some minimal surfaces that can be seen as copies of a triply periodic minimal surface related by reflections in parallel planes. We call them *minimal twin surfaces* for the resemblance with crystal twinning. Twinning of Schwarz' Diamond and Gyroid surfaces are observed in experiment by material scientists. In this paper, we investigate twinings of rPD surfaces, a family of rhombohedral deformations of Schwarz' Primitive (P) and Diamond (D) surfaces, and twinings of the Gyroid (G) surface. Small examples of rPD twins have been constructed in Fijomori and Weber (2009), where we observe non-examples near the helicoid limit. Examples of rPD twins near the catenoid limit follow from Traizet (2008). Large examples of rPD and G twins are numerically constructed in Surface Evolver. A structural study of the G twins brings new insights into the G surface, based on which we speculate a new path of embedded TPMS connecting the G surface to the D surface.

## 1. INTRODUCTION

In material science, a *crystal twinning* refers to a symmetric coexistence of two or more crystals related by Euclidean motions. The simplest situation, namely the *reflection twin*, consists of two crystals related by a reflection in the boundary plane.

*Triply periodic minimal surfaces* (TPMS) are minimal surfaces with the symmetries of crystals. They are used to model lyotropic liquid crystals and many other structures in nature. Recently, Han et al. [HXBC11] synthesized mesoporous crystal spheres with polyhedral hollows. A crystallographic study shows a structure of Schwarz' D (diamond) surface. Most interestingly, twin structures are observed at the boundaries of the domains; see Figure 1. In the language of crystallography, the twin boundaries are  $\{111\}$  planes. We also notice Figure 7.1(b) in [HBL<sup>+</sup>96], which seems like another evidence, but did not catch the attention. Han et al. [HXBC11] also observed twinning of Schwarz' G (gyroid) surface with  $\{211\}$  twin boundaries, which was discovered earlier in [VYC<sup>+</sup>12].

However, it is mathematically premature to call the observed structure "minimal twin surface". Despite the common belief and various convincing explanations, the energetic base of mesophased systems forming periodic minimal surfaces is not well understood. Hence we could not say for sure that the observed surface is minimal. Moreover, it is *a priori* not known that a minimal surface with the observed twin structure exists. And even worse, there is not yet a well-defined notion of "minimal twin surface" in mathematics. Because of the analyticity of minimal surfaces, the definition of twinning in physics does not apply to TPMS.

In this note, we report some minimal surfaces that deserve the name "minimal twin surfaces": they can be seen as copies of a TPMS that are symmetric about parallel reflection planes, as polysynthetic crystal twinings.

Our main interest is the twinning of rPD surfaces, a 1-parameter family of rhombohedral deformations of Schwarz D and P (primitive) surfaces. The common symmetries of the rPD surfaces allow an uniform treatment. The rPD twins forms a family of triply periodic minimal surfaces  $\Phi_{t,n}$ , parametrized by a real number  $t > 0$  and an integer  $n > 0$ , with the following properties

- $\Phi_{t,n}$  has vertical symmetry planes (parallel to the  $z$ -axis) reflections in which form a  $(3, 3, 3)$ -triangle group;
- $\Phi_{t,n}$  has horizontal symmetry planes (orthogonal to the  $z$ -axis) reflections in which form an infinite dihedral group.

---

2010 *Mathematics Subject Classification.* Primary 53A10, 49Q05.

*Key words and phrases.* Triply periodic minimal surfaces, Twin lattice, Surface Evolver.

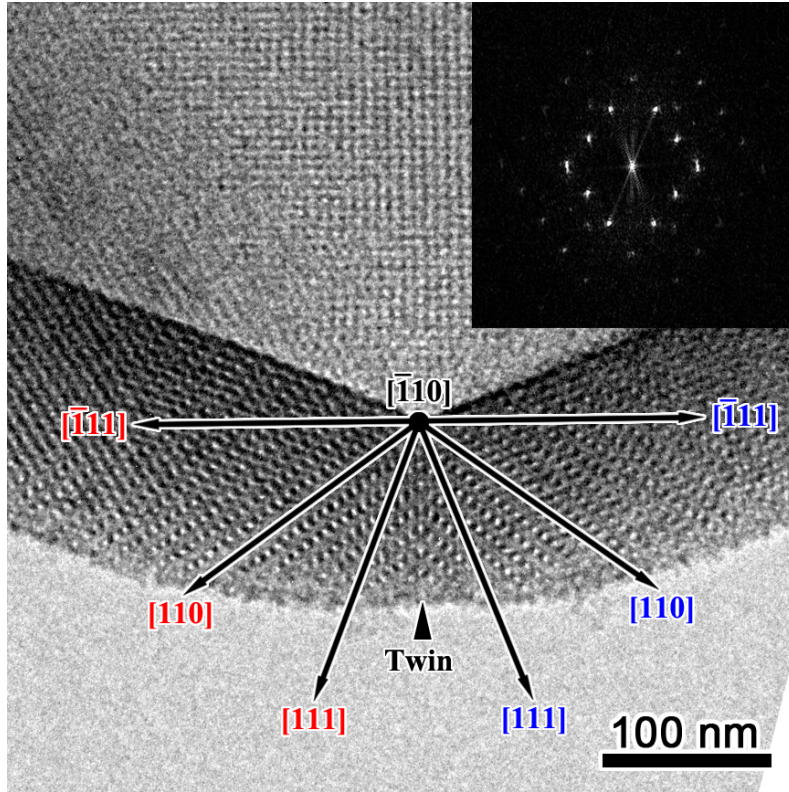


FIGURE 1. Twin structure in minimal D surface observed in experiment. Reuse with permission from Han et al. [HXBC11]. Copyright ©2011 American Chemical Society.

- $\Phi_{t,n}$  modulo the reflectional symmetries is “similar” to the rPD surface with parameter  $t$ .

Examples of rPD twins has been described by Fujimori and Weber [FW09], but the period problem is only solved for small  $n$ . Following their work, we observe that, even when  $n = 3$ ,  $\Phi_{t,n}$  with sufficiently large  $t$  does not exist. On the other hand, for any  $n$ , existence of examples with sufficiently small  $t$  (near the catenoid limit) follows from Traizet [Tra08].

For large  $n$  and  $t$ , exact calculation is very challenging. We then use Brakke’s Surface Evolver [Bra92], an efficient gradient descender, for construction. We obtain a minimal surface if we manage to reduce the integral of squared mean curvature down to practically 0. In this way, we are able to construct  $\Phi_{\sqrt{1/2},n}$  (D twin) numerically for  $n$  as large as 299. In particular, it is now reasonable to believe that the D twin observed in experiment is indeed a minimal twin surface. If  $t$  and  $n$  are too large, our calculation is inconclusive.

We also construct in Surface Evolver twinings of the G surface as observed in experiment. A structural analysis of G twins leads to a new way to visualize and construct the G surface. Based on this new understanding, we speculate mG, a 3-dimensional family of monoclinic deformations of the G surface. In particular, the alleged mG family seems to contain the tD family.

This note is organized as follows. In Section 2 we discuss the symmetries of TPMS twinning in analogy with crystal twinning. Despite the lack of formal definitions, these symmetries are the minimum requirement for a surface to be called “minimal twin surface”. In Section 3, we introduce the rPD surfaces, define their twins by Weierstrass representation, and present rigorous examples with small  $n$  (Section 3.3) or small  $t$  (Section 3.4) and numerical examples in Surface Evolver (Section 3.5). The G twins are numerically constructed and described in Section 4, after which we speculate and discuss the mG family.

## ACKNOWLEDGEMENT

This note presents mathematical context and technical details as a complement and extension to another paper in preparation on material science. I would like to thank my collaborators in that project, especially Chenyu Jin, Lu Han and Nobuhisa Fujita, for their help on this note. I'm very grateful to Karsten Groß-Brauckmann for valuable suggestions, to Matthias Weber for his Mathematica programs, and to Han Yu for helpful discussions.

## 2. CRYSTAL TWINNING AND TPMS TWINNING

The term ‘‘TPMS twinning’’ is not mathematically well defined, and we have no intention to give a rigorous general definition, which could be an impossible task. As far as this note is concerned, the term ‘‘minimal twin surface’’ refers to any minimal surface that is similar to a polysynthetic twin crystal, treating TPMS as the crystal. Here, the word ‘‘similar’’ is open for interpretations, but some rules should be followed. In this section, we summarise the symmetries that we expect for a minimal twin surface, in analogy with crystal twinning.

In physics, a crystal is modeled by a *Bravais lattice*, which can be defined as a discrete point set  $\Lambda \subset \mathbb{R}^3$  invariant under three linearly independent translations. A *lattice plane* of  $\Lambda$  is a plane  $H$  such that  $H \cap \Lambda$  is non-empty and invariant under two linearly independent translations (hence a 2-dimensional lattice). We say that  $H$  is *trivial* if  $\Lambda$  is symmetric about  $H$ . The *reflection twin* of  $\Lambda$  about a non-trivial lattice plane  $H$  consists of lattice points of  $\Lambda$  on one side of  $H$ , and their reflective images on the other side. We call  $H$  the *twin boundary*. Bravais lattice is however an idealized model. In reality, twinning a lattice will introduce inhomogeneity to the energy, hence atoms near the twin boundary will be slightly pulled away from their original positions.

In mathematics, a lattice  $\Lambda$  may be seen as a discrete group acting on  $\mathbb{R}^3$  by translations. A *triply periodic minimal surface* (TPMS)  $P \subset \mathbb{R}^3$  is an *oriented* minimal surface invariant under the action of a lattice. The fundamental domain of translational symmetries of  $P$  is called the *translational unit*<sup>1</sup>. A plane  $H$  is a *lattice plane* of  $P$  if  $H \cap P$  is invariant under the action of a 2-dimensional lattice, and  $H$  is *trivial* if  $P$  is invariant under the reflection in  $H$ . Planes parallel to a lattice plane are lattice planes with the same translational symmetries. In this note, we will occasionally use Miller index to denote the directions of lattice planes and lattice vectors; but usually the planes of interest are placed parallel or orthogonal to the  $z$ -axis.

There are several ways to extract a concrete Bravais lattice from a TPMS. For the TPMS that we are interested in, we find it convenient to use flat points as lattice points. It is possible that a TPMS lattice plane contains no flat point, hence not a lattice plane for the Bravais lattice we choose. We use an *offset* to describe the position of a TPMS lattice plane  $H$  relative to the Bravais lattice. The offset of  $H$  varies linearly between in  $[0, 1]$ ; offset 0 means that  $H$  contains flat points, and offset 0.5 indicates that  $H$  is in the middle of two Bravais lattice planes. Moreover, the *separation* of two TPMS lattice planes refers to the number of Bravais lattice planes between them.

Like Bravais lattices, TPMS often admit extra symmetries other than the translations. The *symmetry group* or *space group* of a TPMS  $P$ , denoted by  $\text{Sym}(P)$ , is the group of Euclidean symmetries of  $P$ . The fundamental domain of  $\text{Sym}(P)$  is called the *fundamental unit*<sup>2</sup>. For a lattice plane  $H$  of  $P$ ,  $\text{Sym}(H)$  denotes the group of symmetries of  $H \cap P$  induced by the symmetries in  $\text{Sym}(P)$ . Parallel lattice planes have the same symmetry.

We could imitate the definition of crystal twinning in physics: take the part of  $P$  on one side of  $H$  and reflect it to the other side. However, as long as  $H$  is non-trivial, the surface obtained is usually not smooth on the twin boundary, hence definitely not a minimal surface. Local minimization of the area functional will inevitably cause a perturbation near the twin boundary. In this sense, TPMS seems more realistic than Bravais lattices. However, it is very difficult to come up with a formal yet general definition.

As in the case of crystal twinning, we expect the reflection twin of  $P$  about  $H$  to be invariant under the action of  $\text{Sym}(H)$ . In particular,  $\text{Sym}(H)$  contains a 2-dimensional lattice, hence

<sup>1</sup>The crystallographic term is ‘‘primitive unit cell’’.

<sup>2</sup>The crystallographic term is ‘‘asymmetric unit’’.

Let  $P \subset \mathbb{R}^3$  be a triply periodic minimal surface, and  $H$  be a non-trivial lattice plane of  $P$ . A *reflection twin* of  $P$  (or a  $P$  *twin*) about  $H$  is a doubly periodic minimal surface  $\Phi$  that is invariant under the action of  $\text{Sym}(H)$  and under the reflection in  $H$ .

A reflection twin with a single reflection plane  $H$  is aperiodic in the direction orthogonal to  $H$ . This is inconvenient for numerical calculations as computers do not really understand infinity. We will work with *polysynthetic twins* with parallel reflection planes.

Let  $P \subset \mathbb{R}^3$  be a triply periodic minimal surface, and  $H$  be a non-trivial lattice plane of  $P$ . A *polysynthetic twin* of  $P$  (or a  $P$  *twin*) about  $H$  is a triply periodic minimal surface  $\Phi_n$  that is invariant under the action of  $\text{Sym}(H)$  and under the reflection in  $H$  and in another lattice plane  $H'$  parallel to  $H$ .

A polysynthetic twin has infinitely many parallel reflection planes. The subscript  $n$  indicates the smallest separation between these twin boundaries. In the following, the word ‘‘polysynthetic’’ will be omitted unless otherwise stated.

At the moment, for the lack of a formal definition, any minimal surface admitting the symmetries above and locally close (in any reasonable sense) to a TPMS, would be accepted as a minimal twin surface.

### 3. THE rPD TWIN SURFACES

**3.1. The rPD surfaces.** The rPD-family is a 1-parameter family of TPMS with rhombohedral symmetries generalizing Schwarz’ D and P surfaces. A Weierstrass representation for the translational unit of an rPD surface is given by [Fog93, FH99]

$$P_t: \omega \mapsto \text{Re} \int^\omega (1 - z^2, i(1 + z^2), 2z)R(z) dz,$$

where  $\omega \in \mathbb{C}$  and

$$(1) \quad R(z) = [z(z^3 - t^3)(z^3 + t^{-3})]^{-1/2},$$

and  $t > 0$  is the parameter. The Schwarz’ D and P surfaces are restored with  $t = \sqrt{1/2}$  and  $t = \sqrt{2}$ , respectively. The rPD-family is self-conjugate; the conjugate surface of  $P_t$  is  $P_{1/t}$ .

The Weierstrass data given in (1) is first obtained by Meeks [Mee90]; see also [FH92a, FH92b]. In fact, Meeks discovered a 5-dimensional family of TPMS. For a surface in Meeks’ family, the Gauss map represents the translational unit as a two-sheeted cover of  $\mathbb{S}^2$  with four antipodal pairs (eight in total) of simple branch points. The branch points correspond to the flat points on the surface. For instance, after a stereographic projection onto the complex plane  $\mathbb{C}$ , the branch points of  $P_t$  are the roots of  $R(z)^{-2}$ .

The Weierstrass data reflects the symmetries of the rPD surfaces. More specifically, the surface has vertical symmetry planes (parallel to the  $z$ -axis). The group generated by these reflections is the Euclidean triangle group with parameters  $(3, 3, 3)$ . Weyhaupt [Wey06, Theorem 3.14] proved that an embedded TPMS of genus 3 with these symmetries must be an rPD surface or an H surface.

We recommend the following way to visualize rPD surfaces. Consider two equiangular triangles that intersect the  $z$ -axis perpendicularly at their centers, whose projections on the  $xy$  plane differ by a rotation of  $\pi/3$ . Our building block, which we call *catenoid unit*, is the ‘‘catenoid’’ spanned by the two triangles. The whole surface is obtained by order-2 rotations about the edges of the triangles. In the case of D and P surfaces, the  $z$ -axis is in the [111]-direction of the cubic lattice. If the projections of the triangles coincide on the  $xy$  plane, then the same construction yields an H surface. Catenoid units of H surfaces will appear on the twin boundaries of rPD twins.

The 1-parameter family is obtained by ‘‘stretching’’ the two triangles along the  $z$ -axis. Let  $h(t)$  denote the height of the catenoid unit (vertical distance between the triangles) assuming unit inradii for the triangles, and  $A(t)$  be the area of the catenoid assuming unit total area for two triangles. Using the formulae given in Appendix A of [FH99] (where the parameter  $r_0$  correspond to our  $1/t$ ), we plot  $h$  and  $A$  against  $t$  in Figure 2. The calculations are done in Sage [The16].

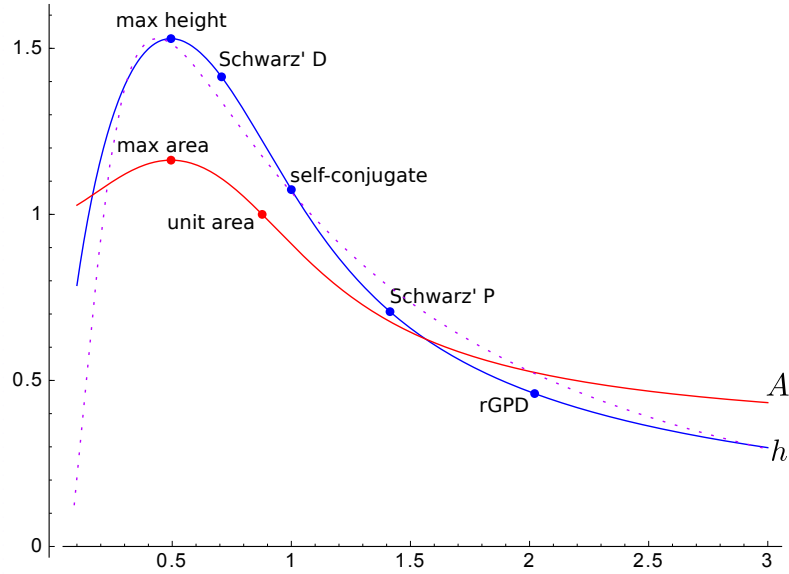


FIGURE 2. Plot of the height  $h$  (solid blue) of a catenoid unit assuming unit inradii for the bounding triangles, and the area  $A$  (solid red) assuming unit total area for the bounding triangles, against the parameter  $t$  on the horizontal axis. The dotted line is the reparameterization of  $h$  with the parameter  $\tau$  in place of  $t$  on the horizontal axis.

The height  $h$  attains its maximum  $h_{\max} = 1.529295 \dots$  at  $t_0 = 0.494722 \dots$  and converges to 0 in both limits  $t \rightarrow \infty$  and  $t \rightarrow 0$ . With a distance bigger than  $h_{\max}$ , the triangles span no catenoid; the only minimal surface is the relative interiors of the triangles. Any  $h < h_{\max}$  corresponds to two different rPD surfaces; the one with bigger  $t$  has smaller area.

The area  $A$  attains its maximum  $S_{\max} = 1.163261 \dots$  at  $t = 0.494893 \dots$  and converges to 1 in the limit  $t \rightarrow 0$ , to  $1/3$  in the limit  $t \rightarrow \infty$ . The area exceeds 1 as long as  $t < t_1 = 0.877598 \dots$ . Hence for  $t$  between  $t_0$  and  $t_1$ , the catenoid is only a local minimizer for the area functional; the relative interiors of the triangles has smaller area.

Other interesting points are:  $t = \sqrt{1/2}$  for the D surface;  $t = \sqrt{2}$  for the P surface;  $t = 1$  is a self-conjugate surface; and  $t = 1/t_0$  is the rGPD surface according to [FH99].

**3.2. A Weierstrass representation of rPD twins.** Fujimori and Weber [FW09] developed an approach to construct surfaces with vertical symmetry planes. Instead of a cover of  $\mathbb{S}^2$ , the Gauss map descends to the quotient torus  $\mathbb{C}/\langle 1, \tau i \rangle$ , where  $\tau \in \mathbb{R}_+$  is an adjustable parameter. For example, the Weierstrass representation of an rPD surface is given by [Wey06, Wey08]

$$P_\tau: \omega \mapsto \operatorname{Re} \int^\omega \left( \frac{1}{2}(G_\tau^{-1} - G_\tau), \frac{i}{2}(G_\tau^{-1} + G_\tau), 1 \right) dz,$$

where the Gauss map

$$G_\tau(z) = \left( \rho \frac{\vartheta(z; \tau)}{\vartheta(z - 1/2 - \tau/2; \tau)} \right)^{2/3}$$

is defined on the torus  $\mathbb{C}/\langle 1, \tau i \rangle$ . Here,  $\rho$  is the Lopez–Ros factor, and

$$\vartheta(z; \tau) = \sum_{k=-\infty}^{\infty} e^{-\pi(k+\frac{1}{2})^2\tau + 2\pi i(k+\frac{1}{2})(z-\frac{1}{2})}$$

is one of the Jacobi  $\vartheta$ -functions;  $\vartheta(z; \tau)$  has simple zeros at the lattice points spanned by 1 and  $\tau i$ . On the bottom of Figure 3, we show the zeros and poles of  $G_\tau$ . They correspond to points of  $P_\tau$  with vertical normal vectors; these are exactly the flat points of  $P_\tau$ , and lie on the intersections of the vertical symmetry planes.

Note that  $\tau$  is an equivalent but different parameter as  $t$ . For comparison, the height of the catenoid unit is plotted against  $\tau$  by a dotted curve in Figure 2. The plot is generated by Sage [The16], but the calculations are done using mpmath [J<sup>+</sup>13]. The Schwarz' P surface is restored with  $\tau = 1.563401 \dots$  [Wey06]. The relation between conjugate surfaces is similar: the conjugate surface of  $P_\tau$  is  $P_{1/\tau}$ .

Apart from the vertical reflection planes, horizontal reflection planes are assumed in [FW09] in order to take advantage of the symmetry. Up to a translation, we may assume that one horizontal symmetry plane correspond to the imaginary axis of  $\mathbb{C}$ .

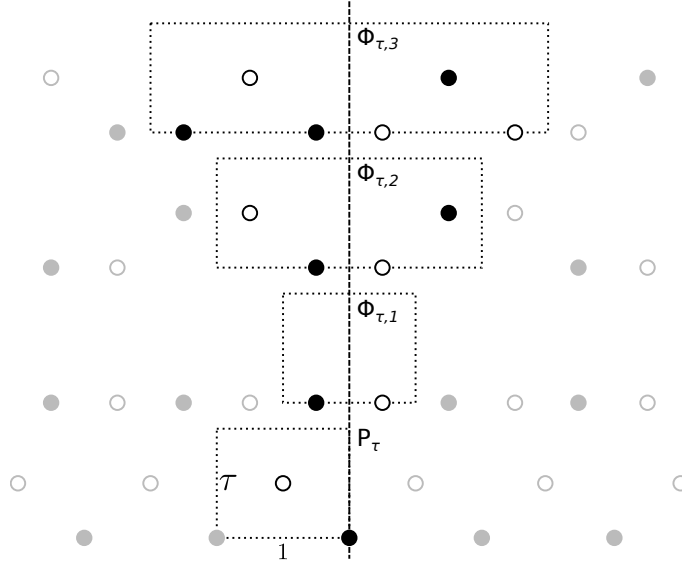


FIGURE 3. Zeros (filled circles) and poles (empty circles) of the Gauss maps  $G_\tau$  and  $G_{\tau,n}$ ,  $n = 1, 2, 3$ . The dotted rectangles indicate the tori on which the Gauss maps are defined.

Following the argument in [FW09], we define the rPD *twin surface*  $\Phi_{\tau,n}$  by the Weierstrass representation

$$\Phi_{\tau,n} : \omega \mapsto \operatorname{Re} \int^\omega \left( \frac{1}{2}(G_{\tau,n}^{-1} - G_{\tau,n}), \frac{i}{2}(G_{\tau,n}^{-1} + G_{\tau,n}), 1 \right) dz,$$

where the Gauss map

$$G_{\tau,n}(z) = \rho \prod_{k \text{ odd}} \left( \frac{\vartheta((z - p_k)/n; \tau/n)}{\vartheta((z + p_k)/n; \tau/n)} \right)^{2/3} \prod_{k \text{ even}} \left( \frac{\vartheta((z - p_k - \tau/2)/n; \tau/n)}{\vartheta((z + p_k - \tau/2)/n; \tau/n)} \right)^{-2/3},$$

and  $(p_k)_{1 \leq k \leq n}$  are real numbers such that  $0 < p_1 < p_2 < \dots < p_n < n/2$  and  $p_k + p_{n+1-k} = n/2$ .

Note that we scale the  $\vartheta$ -function by  $1/n$  so that the zeros and poles of  $G_{\tau,n}$  are “close” to those of  $G_\tau$  within half of the torus  $\mathbb{C}/\langle 1, n\tau i \rangle$ ; see Figure 3. The Lopez–Ros factor  $\rho$  is fixed to 1 so that  $|G_{\tau,n}(z)| = 1$  for all  $z \in i\mathbb{R}$ ; see Appendix A of [Wey06].

**3.3. Example and non-examples of small  $n$ .** The fact that  $\Phi_{\tau,n}$  satisfies the expected symmetries follows from [FW09]. But to prove their existence, we need to solve the period problem. In our case, the period problem for  $\Phi_{\tau,n}$  asks to find  $p_k$  such that

$$\operatorname{Re} \int^{p_k} \left( \frac{1}{2}(G_{\tau,n}^{-1} - G_{\tau,n}), \frac{i}{2}(G_{\tau,n}^{-1} + G_{\tau,n}) \right) dz$$

are vertices of an equiangular triangle. In [FW09], the period problem is solved for small  $n$ 's, as an answer is immediate by symmetry. When  $n = 1$  we have  $p_1 = 1/4$ ; this is an H surface. When  $n = 2$ , we have  $p_1 = 1/4$  and  $p_2 = 3/4$ ; this is Karcher's T-WP surface.

For  $n = 3$ , the period problem is 1-dimensional. Examples of  $\Phi_{t,3}$  are computed numerically. The Mathematica program for this purpose is kindly provided to us by Matthias Weber. The period problem asks to solve the following equations:

$$(2) \quad \begin{aligned} & \operatorname{Re} \int_0^{3/2+\tau/2} \frac{i}{2} (G_{\tau,3}^{-1} + G_{\tau,3}) dz = 0 \\ & \cos \frac{\pi}{6} \operatorname{Re} \int_{\tau/2}^{3/2} \frac{1}{2} (G_{\tau,3}^{-1} - G_{\tau,3}) dz + \sin \frac{\pi}{6} \operatorname{Re} \int_{\tau/2}^{3/2} \frac{i}{2} (G_{\tau,3}^{-1} + G_{\tau,3}) dz = 0 \end{aligned}$$

Under the symmetric assumptions  $p_2 = 3/4$  and  $p_1 + p_3 = 3/2$ , the lhs of the equations are actually the same.

When we change  $\tau$  to a very large value, Mathematica can not find any root. In Figure 4 we plot the lhs of (2) against  $p_1/3$  for six values of  $\tau$ , which clearly shows absence of solution for  $\tau \geq 3$ . In these plots we allow  $p_1 > p_2 = 3/4$ , in which case  $p_1$  should be understood as  $p_3$ ; the horizontal reflectional symmetry is then obvious. One observes that, as  $\tau$  increases,  $p_1$  and  $p_3$  are pushed towards the center  $p_2 = 3/4$ , finally meet there and vanish. We calculate that  $p_1 = p_2 = p_3 = 3/4$  when  $\tau = 2.916517 \dots$ .

**Observation 1.** *There is a real number  $T > 0$  such that the period problem for  $\Phi_{t,3}$  has no solution for  $t > T$ .*

This observation is no surprise. The smaller the parameter  $t$  is, the closer the catenoid unit is to a standard catenoid. A standard catenoid has a natural horizontal symmetry plane, hence it is easier to twin  $P_t$  for small  $t$ . In the other limit  $t \rightarrow \infty$ , helicoids are forming. As the only properly embedded simply connected non-planar minimal surface in  $\mathbb{R}^3$  [MR05], it is not possible to twin the standard helicoid. Hence twinning  $P_t$  with large  $t$  is expected to be difficult or impossible.

Another way to understand the situation is the following: On the one hand, when  $t$  is large,  $P_t$  is far from perpendicular to the horizontal planes. Hence to meet the free boundary condition on the twin boundaries, a larger perturbation would be needed. Under the perturbation, the flat points at height  $p_1$  and  $p_3$  is moving vertically towards  $p_2$ . On the other hand, the flat points are already very close in the  $z$  direction, and there is little space for perturbation. These two factors together eliminates the possibility of twinning rPD surfaces with large  $t$ .

Numerical solution for larger  $n$  is challenging. But it is now reasonable to conjecture that

**Conjecture 1.** *There is a monotonically decreasing function  $T(n) > 0$ ,  $n \geq 3$ , such that the period problem for  $\Phi_{t,n}$  has no solution for  $t > T(n)$ .*

**3.4. Examples of small  $t$ .** In the other end, for any  $n$ , the period problem is solved by Traizet [Tra08] for sufficiently small  $t$ . We now introduce his work.

Traizet was interested in TPMS with periods  $(T_1, 0)$ ,  $(T_2, 0)$  and  $(T_3, \varepsilon)$  which looks like infinitely many horizontal planes  $H_0, H_1, \dots$  with  $H_0$  at  $z = 0$  and  $H_N$  at  $z = \varepsilon$ , and adjacent planes are connected by small catenoid necks. As  $\varepsilon$  tends to 0, such a TPMS converges to a countably sheeted plane, and the catenoid necks converges to singular points arranged in the lattice spanned by  $T_1$  and  $T_2$ . We identify the plane to  $\mathbb{C}$  so that we can talk about positions and periods by complex numbers. Let  $m_k$ ,  $0 \leq k < N$ , be the number of catenoid necks between  $H_k$  and  $H_{k+1}$  and  $p_{k,i}$ ,  $1 \leq i \leq m_k$ , be the limit position of the  $i$ -th catenoid neck. The collection of  $\{p_{k,i}\}$  together with the periods  $T_1, T_2, T_3$  is called a *configuration*.

Given a configuration, Traizet [Tra08] defines the *force* on the  $i$ -th neck between  $H_k$  and  $H_{k+1}$  as follows [Tra08, Section 4.3.1]:

$$(3) \quad \begin{aligned} F_{k,i} = & \sum_{j \neq i} \frac{2}{m_k} \zeta(p_{k,i} - p_{k,j}) \\ & - \sum_{k'=k \pm 1} \sum_j \frac{1}{m_k m_{k'}} \zeta(p_{k,i} - p_{k',j}) \\ & + \frac{1}{m_k} [(2x_k - x_{k-1} - x_{k+1})\eta_1 + (2y_k - y_{k-1} - y_{k+1})\eta_2], \end{aligned}$$

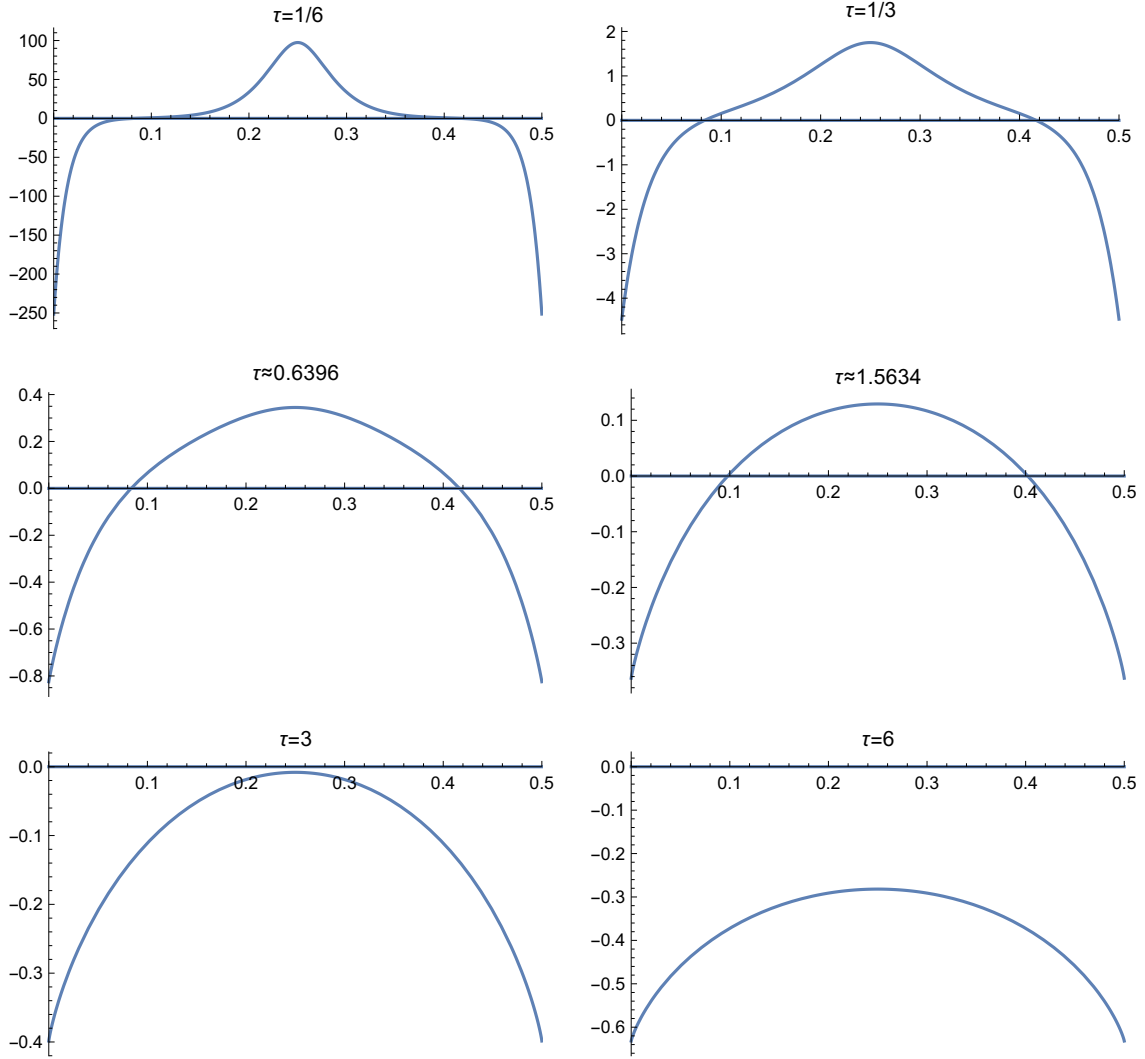


FIGURE 4. Plot of the lhs of (2) against  $p_1/3$  for six different  $\tau$ 's. In the middle row, the left is the twin of D surface, the right is the twin of P surface.

where

$$\zeta(z) = \frac{1}{z} + \sum_{0 \neq w \in \langle T_1, T_2 \rangle} \left( \frac{1}{z-w} + \frac{1}{w} + \frac{z}{w^2} \right)$$

is the Weierstrass  $\zeta$  function;  $\eta_i = 2\zeta(T_i/2)$ ,  $i = 1, 2$ ; and the center of mass  $\sum_j p_{k,j}/m_k = x_k T_1 + y_k T_2$ . The configuration is said to be *balanced* if all the forces  $F_{k,i}$  vanishes, and *non-degenerate* if the differential of the map sending the positions  $\{p_{k,i}\}$  to the forces  $\{F_{k,i}\}$  has real co-rank 2. Traizet [Tra08] proved that, if the configuration is balanced and non-degenerate, then the TPMS described above exists and form a smooth family for sufficiently small  $\epsilon$ .

The rPD surfaces with small  $t$  are examples of Traizet's surfaces; the configuration is given by

$$\begin{aligned} N &= 2, & m_0 &= m_1 = 1, \\ T_1 &= 1, & T_2 &= a = \exp(i\pi/3), & T_3 &= 2(1+a)/3, \\ p_{0,1} &= 0, & p_{1,1} &= (1+a)/3. \end{aligned}$$

The balance and non-degeneracy has been proved in [Tra08, Section 4.3.3]; see also Proposition 3 of the same paper.

The H surfaces are also examples; the only difference from the rPD surfaces is  $T_3 = 0$ . To verify Traizet's force balancing condition, consider the three integral of  $\zeta'(z) = -\wp(z)$  along the directed segments shown in Figure 5. The Weierstrass elliptic function  $\wp(z)$  is even and invariant under the action of  $\langle 1, a \rangle$ . The integrals sum up to 0 because of the symmetries. Therefore,

$$\left[ \zeta\left(\frac{1+a}{3}\right) - \zeta\left(\frac{1}{2}\right) \right] + \left[ \zeta\left(\frac{1+a}{3}\right) - \zeta\left(\frac{a}{2}\right) \right] + \left[ \zeta\left(\frac{1+a}{3}\right) - \zeta\left(\frac{1+a}{2}\right) \right] = 0.$$

Since  $\zeta\left(\frac{1}{2}\right) + \zeta\left(\frac{a}{2}\right) = \zeta\left(\frac{1+a}{2}\right)$ , we conclude that

$$-2\zeta\left(\frac{1+a}{3}\right) + \frac{4}{3}\zeta\left(\frac{1}{2}\right) + \frac{4}{3}\zeta\left(\frac{a}{2}\right) = 0.$$

Hence the configuration is balanced. The non-degeneracy is verified numerically.

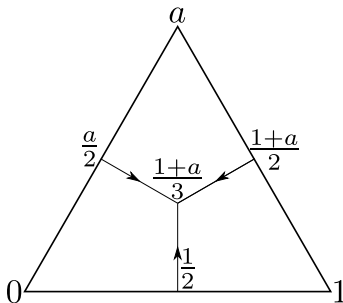


FIGURE 5. The integrals of  $\zeta'(z) = -\wp(z)$  along the three directed segments sum up to 0 because of the symmetry. This proves the force balancing condition for the H surfaces.

At this point, crystallographers should notice the analogy of rPD and H family with the cubic and hexagonal closed packings. Within a period, there are three possible limit positions for the necks, namely  $j(1+a)/3$  with  $j = 0, 1, 2$ . We then obtain an infinite sequence consisting of letters 0, 1 and 2. The rPD surfaces has a periodic sequence  $\dots 012012012 \dots$ . The sequences for rPD twins should be periodic and palindromic, like  $\dots 010101010 \dots$  for the H surface,  $\dots 012101210 \dots$  for the T-WP surface, etc.

The formula (3) only involves adjacent layers. Up to symmetry, the only possible consecutive triples is 012 and 010, for which the force balancing condition has been verified in rPD and H surfaces. Hence the rPD twin configurations are all balanced and non-degenerate. Consequently, for any  $n > 0$ , there is a real number  $\epsilon_n > 0$  such that the minimal twin surface  $\Phi_{\tau, n}$  exists for  $0 < \tau < \epsilon_n$ . In fact, the argument works for any periodic sequence. For example, the sequence  $\dots 0101201012 \dots$  also satisfy the force balancing condition.

Traizet's proof uses implicit function theorem. We do not know if there is a universal  $\epsilon > 0$  such that  $\Phi_{\tau, n}$  are embedded for any  $n > 0$  and  $0 < \tau < \epsilon$ .

**3.5. Numerical examples with Surface Evolver.** Brakke's Surface Evolver [Bra92] is a software that simulates the physics of surfaces by minimizing energies. Surfaces are modeled by triangulations, and the energy is minimized by gradient descent method. Surface Evolver can handle various energies under various constraints.

In an usual application, the energy to minimize is the surface tension energy or the area functional. However, contrary to the intuition of many, TPMS do not result from area minimization. In the translational unit, a TPMS is actually a strict maximum of the area functional among its parallel surfaces [GB12]. A TPMS is indeed stable for the area functional if a volume constraint is imposed in the translational unit [GBW96]. But this is again false for any slightly larger piece [Ros92]. Modulo the reflectional symmetries,  $\Phi_{t, n}$  correspond to a large piece of  $P_t$ , hence the area functional is not our option.

We will minimize instead the Willmore energy, or more precisely, the integral of the squared mean curvature; see [HKS92] for Surface Evolver experiments on this energy. Physically, the

Willmore energy measures the deviation of the surface from the zero mean curvature, hence models the “bending” energy. The Willmore energy vanishes on minimal surfaces.

We generate the rPD twin surface  $\Phi_{t,n}$  in Surface Evolver in four steps:

- (1) Prepare a catenoid unit.

Let  $h = h(t)$  be the height function defined in Section 3.1. Consider four points

$$A(1, 0, 0), B(-1/2, \sqrt{3}/2, 0), C(-1, 0, h), D(1/2, \sqrt{3}/2, h).$$

The catenoid unit of  $P_t$  modulo reflectional symmetries is a minimal surface with fixed boundary conditions on the segments  $AB$  and  $CD$ , and free boundary conditions on the vertical planes  $y \pm \sqrt{3}x = \sqrt{3}$ . Reflections in these planes yield the whole catenoid unit. The boundary triangles has unit inradius, compatible with the discussions in Section 3.1. The unit is obtained in Surface Evolver by minimizing the area functional. As a consequence of this practice, we can only obtain rPD surfaces with parameter  $t > t_0 = 0.494722 \dots$ .

- (2) Generate a segment.

We generate a segment of  $P_t$  from the catenoid unit by order-2 rotations about the segment  $AB$  or  $CD$ . In Surface Evolver, this is done by listing the matrices, say  $\mathbf{a}$  and  $\mathbf{b}$ , of the two rotations in `VIEW_TRANSFORM_GENERATORS`. Assume an odd  $n$ , we set `transform_expr` to be a string  $k(\mathbf{ba})$  if  $n = 4k - 1$  or  $k(\mathbf{ba})\mathbf{b}$  if  $n = 4k + 1$ . Then the Surface Evolver will display  $n + 1$  catenoid unit. Finally, we use the `detorus` command to convert the displayed segment unit into a real surface.

- (3) Slice the segment.

In this step, we use Brakke’s script `slicer.cmd`. It is included in the Evolver distribution, and also available on the website of Surface Evolver. It removes the part of the surface on one side of a given plane. We slice the segment in the previous step by two horizontal planes at offset 0.5 and separation  $n$ . The script also marks the vertices and edges newly created by the slice. This allows us to impose free boundary conditions by constraining the new vertices and edges on the slicing planes.

- (4) Evolve the surface.

We turn off the surface tension energy (`set facet tension 0`), and turn on the Willmore energy, which is the integral of squared mean curvature. Then we leave Evolver to minimize the energy. Apart from the command `g` that does one step of gradient descent, the command `hessian_seek` is particularly useful in this step to accelerate the calculation. If the Willmore energy decreases to practically 0, we obtain a minimal surface with free boundary condition on the boundary of a triangular prism. Reflections in the faces of the prism give the whole  $\Phi_{t,n}$ .

In Figure 6, we show the result of each step with  $t = \sqrt{2}$  (Schwarz’ P surface) and  $n = 3$ .

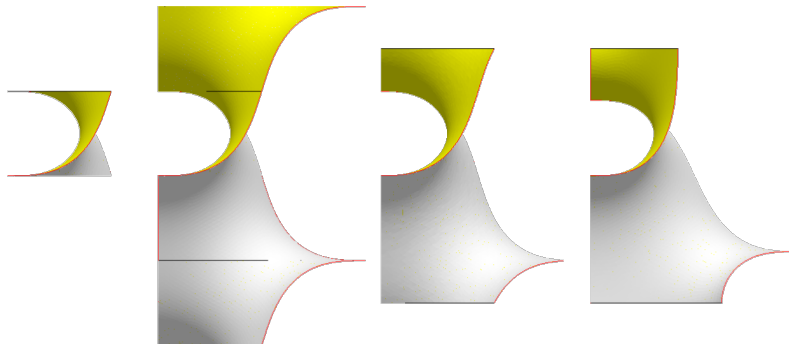


FIGURE 6. Result of each step with  $t = \sqrt{2}$  and  $n = 3$ .

The program can be easily modified to change the parameters  $t$  and  $n$ . We perform calculations for parameters  $t = t_0, \sqrt{1/2}$  (D),  $1, \sqrt{2}$  (P), and  $n = 1$  (H),  $3, 5, 11, 21, 99$ . When  $n$  is big, the last step will be very slow. We can increase the speed in the price of precision by reducing the number

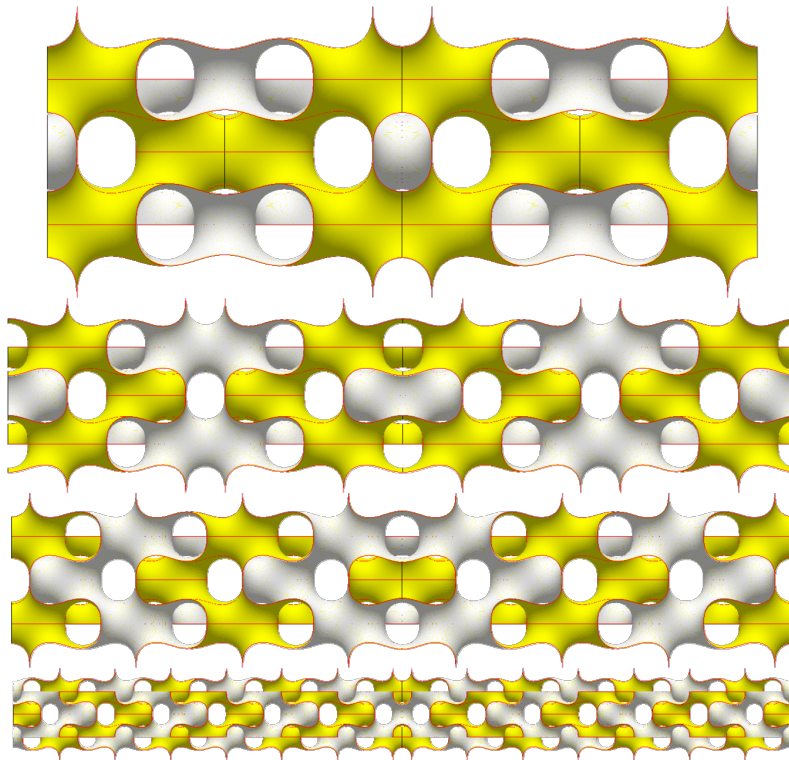


FIGURE 7. D twin surfaces ( $t = \sqrt{1/2}$ ). From top to bottom,  $n = 3, 5, 11, 21$ . The twin boundary is clearly seen in the middle.

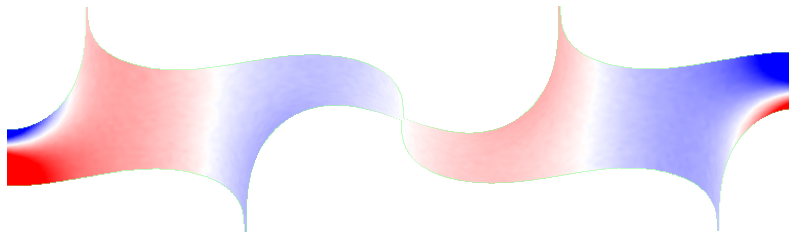


FIGURE 8. Deviation of the D twin with  $n = 5$  from the D surface. Blue and red indicate perturbations in opposite directions; white indicates coincidence.

of faces in the catenoid unit. In Surface Evolver, the command `r` refines the surface by subdividing each triangle into four. When generating the catenoid unit, we refine five times for  $n = 1, 3, 5$ , four times for  $n = 11, 21$  and three times for  $n \geq 99$ .

The calculation goes surprisingly smooth for small  $t$  and small  $n$ . For  $t = t_0$  and  $t = \sqrt{1/2}$  (D), the Willmore energy decreases quickly to the order of  $10^{-26}$  or lower, even when  $n = 99$ . In view of the discussion in Section 3.3, it is reasonable to believe that the calculation would be even faster for smaller  $t$ . The results for  $t = \sqrt{1/2}$  and  $n = 3, 5, 11, 21$  are shown in Figure 7. The difference from the D surface is not visible with human eyes, hence we use CloudCompare [GM<sup>+</sup>16] to calculate the deviation from the D surface; the result for  $n = 5$  is colored accordingly in Figure 8. We can see that the perturbation decays away from the twin boundaries, and the flat points are perturbed towards the middle. These pictures justify that the structure observed in [HXBC11] is indeed a minimal D twin.

**Observation 2.** *The rPD twin surfaces  $\Phi_{t,n}$  exist for a large set of parameters.*

In fact, if we obtain a minimal surface, the calculation roughly solves the period problem. More specifically, the vertices transformed from  $A$  or  $C$  when we generate the segment are the flat points, corresponding to the poles and zeros of the Gauss map  $G_{\tau,n}$ . After normalization, the heights of these points give the sequence  $(p_k)_{1 \leq k \leq n}$ . For example, the  $\Phi_{\sqrt{1/2},3}$  (D twin) generated by Surface Evolver has twin boundaries at  $z = \pm 3\sqrt{2}/2$ , and the surface intersects the lateral edges of the prism at  $z \approx 0$  and  $z \approx \pm 1.41240$ . By a scaling and a translation, we may place the boundaries at  $z = 0$  and  $z = 3/2$ , and obtain  $p_1 \approx 0.25064$ ,  $p_2 \approx 0.75$  and  $p_3 \approx 1.24936$ . Compared to the solution given by the Mathematica program used for [FW09], these values are accurate until the fifth digit after the decimal point. However, the precision is not guaranteed as  $t$  increases. The  $\Phi_{\sqrt{2},3}$  (P twin) shown in Figure 6 gives  $p_1 \approx 0.303350$ ,  $p_2 \approx 0.75$  and  $p_3 \approx 1.196651$ , while Mathematica computes more precisely  $p_1 = 0.293406\dots$ ,  $p_2 = 0.75$  and  $p_3 = 1.20659\dots$ .

The Willmore energy also decreases to the order of  $10^{-26}$  for  $t = 1$  with  $n \leq 21$ , and for  $t = \sqrt{2}$  with  $n \leq 3$ . However, for  $t = 1$  and  $n = 99$ , the Surface Evolver only manages to reduce the Willmore energy to the order of  $10^{-8}$ ; then the decrement becomes extremely slow. For  $t = \sqrt{2}$  (P surface) and  $n = 5$ , the energy seems to stabilize at the order  $10^{-4}$ . These calculations are therefore inconclusive.

**Observation 3.** *Surface Evolver does not converge to a minimal surface if  $t$  and  $n$  is too large.*

We then append more calculations for  $t = \sqrt{1/2}$  to see if it eventually fails with sufficiently large  $n$ . It turns out that we are able to obtain a minimal surface with  $n \leq 299$ . Since the calculation is very time consuming for large  $n$ , we did not perform further computation. But the success with large D twins ensures that the inconclusive results for P twins do not arise from numerical or system errors. Hence we conjecture that  $\Phi_{\sqrt{2},5}$  does not exist, and more generally:

**Conjecture 2.** *There is a monotonically decreasing function  $N(t)$ , such that the period problem for  $\Phi_{t,n}$  has no solution for  $n > N(t)$ .*

We do not rule out the possibility that  $N(t) = \infty$  for sufficiently small  $t$ . If this is the case, we could use a sequence of polysynthetic twins to approximate the reflection twin.

## 4. G TWIN SURFACES

**4.1. Numerical examples with Surface Evolver.** Twinnings of the G surface are also observed in experiment. Taking the flat points as lattice points, the twin boundaries are  $\{211\}$  planes at offset 0. We follow a similar procedure to generate G twin surfaces in Surface Evolver.

- (1) Prepare the G surface in an orthorhombic cell.

Unlike the rPD surfaces, the G surface contains no straight line, and has no symmetry plane. A datafile of initial triangulation is prepared by Fujita using the `torus` model of Surface Evolver. The orthorhombic unit cell is generated by three vectors in the  $[0\bar{1}1]$ ,  $[\bar{1}11]$  and  $[211]$  directions. For our convenience, we made a small modification to place the  $[211]$  direction on the  $z$ -axis.

Since this unit cell is larger than the translational fundamental cell, it is not safe to minimize the area functional [GBW96]. Hence we prepare the G surface by minimizing the Willmore energy directly.

- (2) Generate a segment.

In the torus model, the command `y 3` duplicates the displayed surface along the  $z$ -axis ( $[211]$ -direction). Repetition of the command for  $k$  times would generate  $2^k$  copies of the orthorhombic cell. We do not `detorus` the surface since we need the double periodicity.

- (3) Slice the segment.

Brakke's script does not work well in the torus model, hence we write our own script to slice the segment by two horizontal planes ( $(211)$  planes) at offset 0, and impose free boundary conditions on the slicing planes.

- (4) Evolve the surface.

The program can be easily modified to adjust the separation  $n$  between the slicing planes (twin boundaries). We perform calculation for  $n = 1, 2, 5, 10, 23$ . In all these cases, we are able to

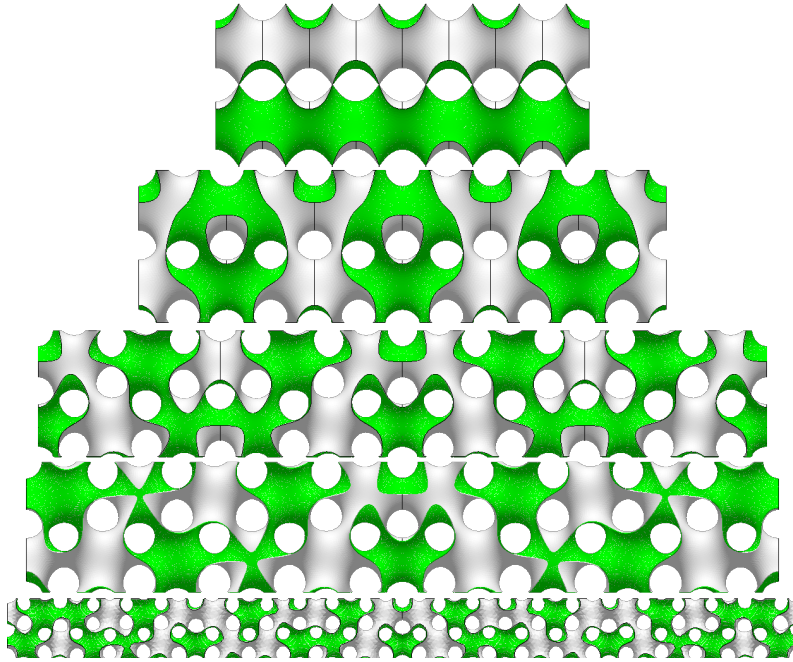


FIGURE 9. G twin surfaces. From top to bottom,  $n = 1, 2, 5, 10, 23$ . The twin boundary is clearly seen in the middle.

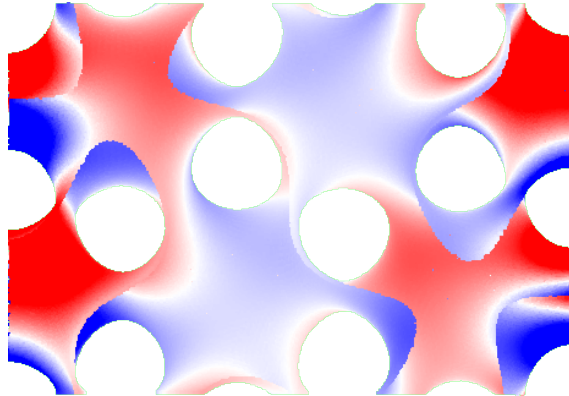


FIGURE 10. Deviation of the G twin with  $n = 5$  from the G surface. Blue and red indicate perturbations in opposite directions; white indicates coincidence.

obtain a minimal surface by reducing the Willmore energy to the order of  $10^{-26}$ . We did not try larger separations. The results are shown in Figure 9. The G twin with  $n = 1$  turns out to be an orthorhombic deformation of the D surface (an oD surface); this will be explained later. In Figure 10, the result for  $n = 5$  is colored according to the deviation from the G surface.

**Observation 4.** *The G twin surfaces exist for a large set of parameters.*

**4.2. A new insight into the G surface.** The Gyroid surface is probably the most beautiful TPMS, but has the reputation of being difficult to visualize. For Surface Evolver, a datafile written by Groß-Brauckmann back in 1995 is still widely used to generate the G surface. It decomposes the cubic unit cell of the G surface into hexagons and rectangles, which is difficult to rewrite from scratch.

The (211) G twins reveal an interesting structure of the G surface which, to the knowledge of the author, was not mentioned before. We show in the upper half of Figure 11 a gyroid sliced by

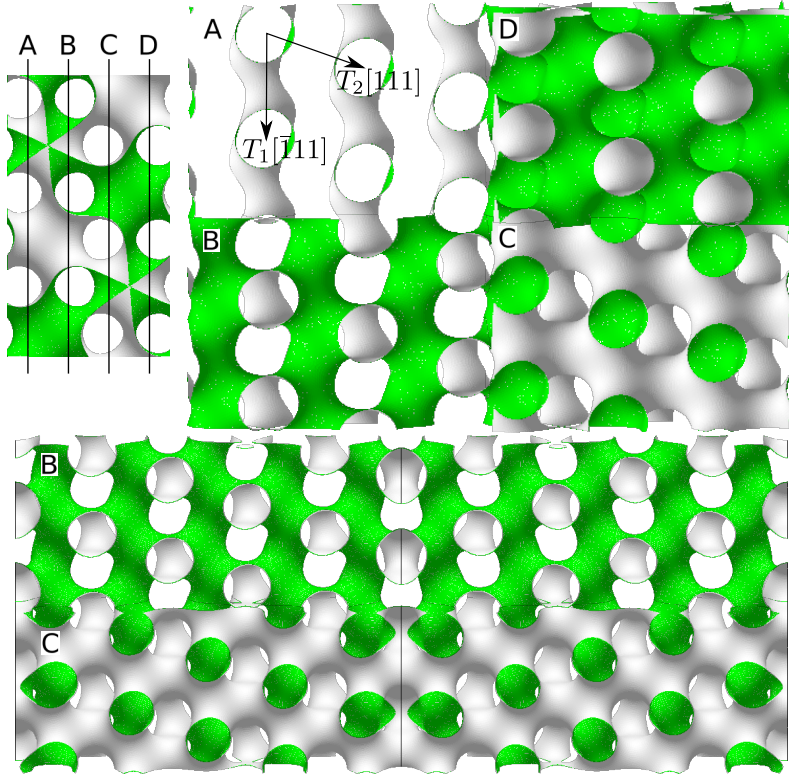


FIGURE 11. The G surface (upper right) and the G twin with  $n = 10$  (bottom) sliced by  $(0\bar{1}1)$  planes at offset 0.5. The position of the slicing planes are indicated in the upper left corner, where the G surface is seen in the  $[\bar{1}11]$  direction.

$(0\bar{1}1)$  planes at offset 0.5. We observe necks arranged in a 2-D lattice. The lattice is spanned by vectors  $T_1[\bar{1}11]$  and  $T_2[111]$ , and the difference between adjacent layers is alternating between  $T_1/2$  and  $T_2/2$ . In the lower half of the same figure, we show the slices of the G twin with  $n = 10$ . We see clearly twinnings of the 2-D lattice, and the twin boundary is parallel to  $T_1$ .

This observation leads to a new way to construct the G surface in Surface Evolver. The initial triangulation in torus model is shown in the upper left corner of Figure 12. The monoclinic unit cell is spanned by  $(\pm\sqrt{2}, 1, 0)$  and  $(0, 0, 2\sqrt{2})$ ; this cell has the same volume as the cubic cell. We prepare four horizontal planes at  $z = j\sqrt{1/2}$ ,  $j = 0, 1, 2, 3$ . Each plane is a 2-torus decomposed into four rhombi, labeled as in the figure. A rhombic tube connects the rhombi  $j$  between plane  $j$  and plane  $j + 1 \pmod{3}$ . After several refinement and evolvment, this simple configuration converges correctly to the G surface by minimizing the Willmore energy; see the evolved result in Figure 12.

It is also possible to start with two horizontal planes in the triclinic unit cell spanned by  $(\pm\sqrt{2}, 1, 0)$  and  $(0, 1, \sqrt{2})$ . Surface Evolver runs faster and better on a smaller unit cell. This construction is successfully implemented with Surface Evolver, but we do not present it here in detail, since it is less straightforward to visualize. Examples will appear in the next section.

**4.3. Monoclinic deformation of the G surface.** We notice that the following configuration is balanced for any linearly independent  $T_1$  and  $T_2$  in  $\mathbb{C}$ , and is generically non-degenerate:

$$(4) \quad \begin{aligned} N &= 2, & m_0 &= m_1 = 1, \\ p_{0,1} &= 0, & p_{1,1} &= T_1/2, \\ T_3 &= (T_1 + T_2)/2. \end{aligned}$$

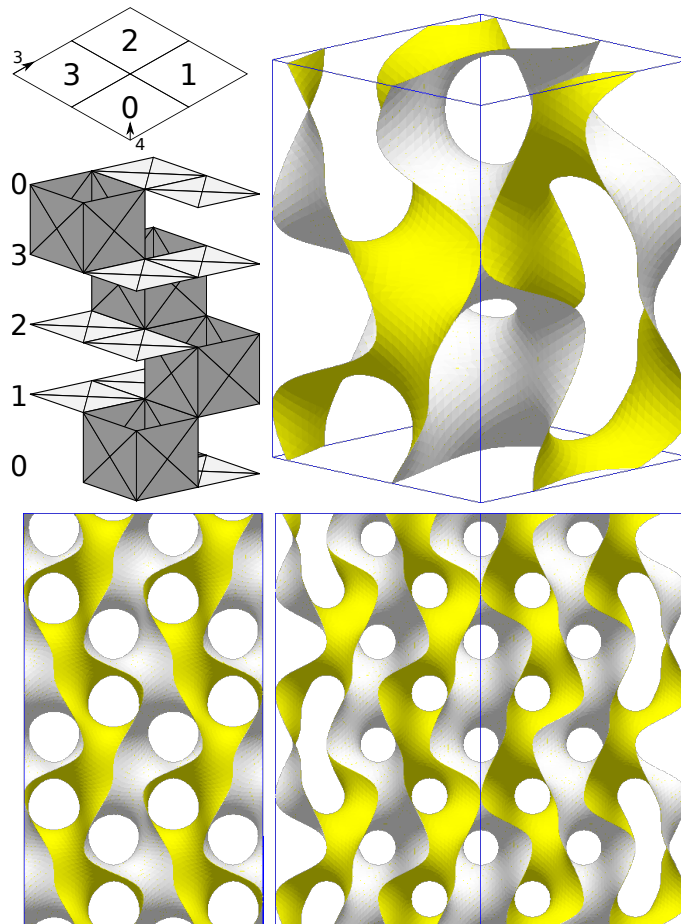


FIGURE 12. A new construction of the Gyroid in Surface Evolver. Upper left: the initial surface consists of four horizontal planes connected by tubes; see text. The small arrows indicates the direction of 3- and 4-fold axis. Upper right: Evolved result in a monoclinic unit cell. Lower left: Evolved result seen along the 3-fold axis. Lower right: Evolved result seen along the 4-fold axis.

In view of our new construction of the G surface, we speculate two kinds of deformations. We can either stretch the G-surface vertically, by changing the vertical distance between horizontal planes; or we can stretch the rhombus horizontally into other quadrangles. We name these alleged deformations the mG family, since the surfaces would have the symmetry of monoclinic lattices. This would be a three dimensional family: one dimension comes from the vertical deformations; the other two from the horizontal deformations.

As for the vertical deformations, it follows from Traizet [Tra08] that the configuration (4) implies a family of TPMS near the catenoid limit, whose horizontal lattice planes admit the same symmetry as the (110) planes of the G surface. We then propose the following conjecture

**Conjecture 3.** *Within the alleged mG family, there is a continuous family of embedded deformations of the G surface that preserve the symmetry of the (011) planes and connects the G surface to the Traizet's surfaces.*

The mG family seems to contain, in particular, all the tetragonal deformations of the D surface (tD family [FH99]). To see this, notice the similarity between configuration (4) with  $T_2 = iT_1$  and the diamond lattice. The (100) planes of the diamond lattice have the symmetry of square lattice, and adjacent (100) planes differ by a half-period in alternating directions.

The 2-D lattice for mG surfaces can be stretched along the diagonal ([100]) into a square of side length 2. We then repeat the program in the previous section with squares of side length 2 in place of the rhombi. The surface evolves into the D surface; see Figure 13. This is very surprising, yet completely reasonable. The other tD surfaces can be achieved by a vertical deformation. Based on this numerical evidence, we conjecture that

**Conjecture 4.** *The alleged mG family includes the tD family as special cases. In particular, the D surface can be directly achieved by horizontally deforming the G surface.*

The deformation we just speculated above provides a path of embedded TPMS that connects the G surface directly to the D surface. It seems different from the tG family [FH99], a path of tetragonal deformations that connects the G surface to the tD surface of parameter 0.43188... (see [FH99] for explanation of the parametrization). Meanwhile, the diagonal of the rhombus happens to be a 4-fold axis of the G surface; and we do observe 4-fold symmetries in the mG deformations in this direction. Moreover, if we stretch too much along the 4-fold axis, such that the rhombus becomes very elongated, we would obtain a 4-fold “saddle tower”. This is again verified with our program; see Figure 13. All these behaviours coincide with the tG family. A comparative study would be necessary to clarify the differences and connections between the tG family and 4-fold mG deformations. Relation between the rG family and 3-fold mG deformations is also of interest.

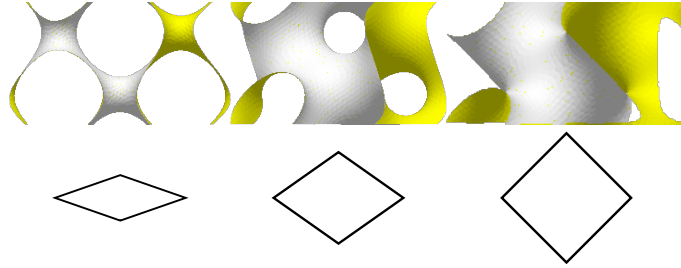


FIGURE 13. The diagonal of the rhombus (vertical in the figure) is a 4-fold axis of the G surface. By stretching the G surface (middle) in this direction, we obtain the D surface (right) and a 4-fold saddle tower (left). The surfaces shown in this figure are in the triclinic unit cell; the 4-fold axis is towards the readers. To be compared with tG surfaces in [FH99, Figure 11].

Near Traizet’s catenoid limit, the mG surfaces can certainly be twinned about horizontal planes; the force balancing condition on the twin boundary is covered in [Tra08, Section 4.3.3], and the condition off the boundary is covered by (4). But in view of the G twin, we are more interested in twinning mG surfaces about vertical planes parallel to  $T_1$ . We performed numerical calculations with  $n = 1, 2, 3$ . However, if we insist that the twin boundaries pass through the catenoid necks, the only balanced configurations turn out to be (4) with  $T_1 = 1$ ,  $T_2 = bi$  or  $T_2 = 1 + bi$ , where  $b = \sqrt{8/9}$ . This is different from what we observed in the G twins; thus our understanding of G twins, and more generally mG twins, is still very limited. Note that the case  $T_2 = bi$  is an orthorhombic deformation of the D surface (oD) as we have observed, which should not be a surprise any more in view of discussions above. For a concrete example of calculation, the configuration for  $n = 1$  is (up to scaling)

$$(5) \quad \begin{aligned} N &= 4, & m_k &= 1 \quad (k = 0 \dots 3), \\ p_{0,1} &= 0, & p_{1,1} &= 1/2, \\ p_{2,1} &= x + 1/2 + bi/2, & p_{3,1} &= x + bi/2, \\ T_1 &= 1, & T_2 &= bi, & T_3 &= 0. \end{aligned}$$

The only solutions for  $F_{0,1} = 0$  are  $x = 0$  and  $x = 1/2$ .

## REFERENCES

- [Bra92] K. A. Brakke, *The surface evolver*, Experiment. Math. **1** (1992), no. 2, 141–165. MR1203871
- [FH92a] A. Fogden and S. T. Hyde, *Parametrization of triply periodic minimal surfaces. I. Mathematical basis of the construction algorithm for the regular class*, Acta Cryst. Sect. A **48** (1992), no. 4, 442–451. MR1170629
- [FH92b] A. Fogden and S. T. Hyde, *Parametrization of triply periodic minimal surfaces. II. regular class solutions*, Acta Cryst. Sect. A **48** (1992), no. 4, 575–591. MR1170629
- [FH99] A. Fogden and S. T. Hyde, *Continuous transformations of cubic minimal surfaces*, The European Physical Journal B-Condensed Matter and Complex Systems **7** (1999), no. 1, 91–104.
- [Fog93] A. Fogden, *Parametrization of triply periodic minimal surfaces. III. General algorithm and specific examples for the irregular class*, Acta Cryst. Sect. A **49** (1993), no. 3, 409–421. MR1228292
- [FW09] S. Fujimori and M. Weber, *Tripoly periodic minimal surfaces bounded by vertical symmetry planes*, Manuscripta Math. **129** (2009), no. 1, 29–53. MR2496955
- [GB12] K. Große-Brauckmann, *Tripoly periodic minimal and constant mean curvature surfaces*, Interface Focus **2** (2012), 582–588.
- [GBW96] K. Große-Brauckmann and M. Wohlgemuth, *The gyroid is embedded and has constant mean curvature companions*, Calc. Var. Partial Differential Equations **4** (1996), no. 6, 499–523. MR1415998
- [GM<sup>+</sup>16] D. Girardeau-Montaut et al., *CloudCompare (Version 2.8.beta)*, 2016. Retrieved from <http://www.cloudcompare.org/>.
- [HBL<sup>+</sup>96] S. Hyde, Z. Blum, T. Landh, S. Lidin, B. W. Ninham, S. Andersson, and K. Larsson, *The language of shape: The role of curvature in condensed matter: Physics, chemistry and biology*, Elsevier, 1996.
- [HKS92] L. Hsu, R. Kusner, and J. Sullivan, *Minimizing the squared mean curvature integral for surfaces in space forms*, Experiment. Math. **1** (1992), no. 3, 191–207. MR1203874
- [HXBC11] L. Han, P. Xiong, J. Bai, and S. Che, *Spontaneous formation and characterization of silica mesoporous crystal spheres with reverse multiply twinned polyhedral hollows*, Journal of the American Chemical Society **133** (2011), no. 16, 6106–6109.
- [J<sup>+</sup>13] F. Johansson et al., *mpmath: a Python library for arbitrary-precision floating-point arithmetic (version 0.18)*, 2013. <http://mpmath.org/>.
- [Mee90] W. H. Meeks III, *The theory of triply periodic minimal surfaces*, Indiana Univ. Math. J. **39** (1990), no. 3, 877–936. MR1078743
- [MR05] W. H. Meeks III and H. Rosenberg, *The uniqueness of the helicoid*, Ann. of Math. (2) **161** (2005), no. 2, 727–758. MR2153399
- [Ros92] M. Ross, *Schwarz' P and D surfaces are stable*, Differential Geom. Appl. **2** (1992), no. 2, 179–195. MR1245555
- [The16] The Sage Developers, *Sagemath, the Sage Mathematics Software System (Version 7.3)*, 2016. <http://www.sagemath.org>.
- [Tra08] M. Traizet, *On the genus of triply periodic minimal surfaces*, J. Differential Geom. **79** (2008), no. 2, 243–275. MR2420019
- [VYC<sup>+</sup>12] S. Vignolini, N. A. Yufa, P. S. Cunha, S. Guldin, I. Rushkin, M. Stefik, K. Hur, U. Wiesner, J. J. Baumberg, and U. Steiner, *A 3d optical metamaterial made by self-assembly*, Advanced Materials **24** (2012), no. 10, OP23–OP27.
- [Wey06] A. G. Weyhaupt, *New families of embedded triply periodic minimal surfaces of genus three in euclidean space*, ProQuest LLC, Ann Arbor, MI, 2006. Thesis (Ph.D.)—Indiana University. MR2709166
- [Wey08] A. G. Weyhaupt, *Deformations of the gyroid and Lidinoid minimal surfaces*, Pacific J. Math. **235** (2008), no. 1, 137–171. MR2379774

FREIE UNIVERSITÄT BERLIN, INSTITUT FÜR MATHEMATIK, ARNIMALLEE 2, 14195 BERLIN, GERMANY  
*E-mail address:* hao.chen.math@gmail.com